JACS
JOURNAL OF THE AMERICAN CHEMICAL SOCIETY

COMMUNICATION

pubs.acs.org/JACS

Proton-Coupled Electron Transfer from Tyrosine: A Strong Rate Dependence on Intramolecular Proton Transfer Distance

Ming-Tian Zhang, Tania Irebo, Olof Johansson, and Leif Hammarström*

Department of Photochemistry and Molecular Science, Uppsala University, Box 523, SE-751 20 Uppsala, Sweden

Supporting Information

ABSTRACT: Proton-coupled electron transfer (PCET) was examined in a series of biomimetic, covalently linked $Ru^{II}(bpy)_3$–tyrosine complexes where the phenolic proton was H-bonded to an internal base (a benzimidazyl or pyridyl group). Photooxidation in laser flash/quench experiments generated the Ru^{III} species, which triggered long-range electron transfer from the tyrosine group concerted with short-range proton transfer to the base. The results give an experimental demonstration of the strong dependence of the rate constant and kinetic isotope effect for this intramolecular PCET reaction on the effective proton transfer distance, as reflected by the experimentally determined proton donor–acceptor distance.

Proton-coupled electron transfer (PCET)[1] is an essential process in chemical and biological catalysis, for example in water splitting,[2] oxygen activation,[3] proton reduction,[4] nitrogen fixation,[5] and ribonucleotide reductase reactions.[6] Furthermore, utilization of solar energy is an area of intense research that is viewed as a promising way to solve the energy problem. In fact, mechanistic insight into PCET is a significant prerequisite for the effective design of powerful catalysts for water splitting and solar fuels generation by artificial photosynthesis. Interestingly, photosystem II (PSII) has provided a template for understanding successful molecular water oxidation catalysis and PCET processes.[2] Oxidation of tyrosine-Z in PSII, where the phenolic proton is transferred to the nearby histidine via a hydrogen bond, supplies the oxidative equivalents to the manganese cluster that are required for water oxidation. These reactions have inspired interest in the PCET oxidation of H-bonded phenols.[7−9] There are two possible types of mechanisms for oxidation of H-bonded tyrosine and its derivatives: *stepwise* and *concerted* pathways. The latter can avoid the involvement of higher-energy intermediates but is less robust with respect to structural change in comparison with the former.[10] Thus, perturbation of the proton transfer distance might provide critical insight into the nature of the coupling between the electron and the proton. Because the proton has a much larger mass than the electron, it is likely that proton tunneling in PCET reactions of synthetic systems needs to be even more carefully designed and controlled than the electron transfer.

Recent work on the oxidation of H-bonded phenols has provided important information about PCET.[7−9] However, there is still a limited amount of experimental data as well as contrasting reports on the relationship between the physicochemical features of the H-bond and the PCET kinetics, such as the effect of geometry, distance, and H-bond strength. Some studies of phenols with external[7g] or internal[7b,c] bases have shown a dependence of the rate on the driving force (given by the pK_a value for the base) but reported no distinguishable effects of, for example, the H-bond length that determines the proton transfer distance. Another study compared two phenols having a pyridine base that was either conjugated with the phenol or linked via a methylene group [**3′** and **4′**; see the Supporting Information (SI)][7d] and instead attributed the relatively rapid oxidation rate of the former to the effect of a resonance-assisted H-bond that was suggested to result in a flatter proton transfer barrier. Our group compared intramolecular PCET in two phenols containing conjugated (salicylic acid) or nonconjugated (*o*-hydroxyphenylacetic acid) carboxylate groups.[8b,c] By theoretical simulation of the kinetic data, we showed that although the H-bond length was very similar in the two compounds, there were differences in, for example, the stiffness of the H-bond that affected the thermal distribution of tunneling distances ("promoting vibrations"; see below) and substantially increased the rate for the salicylic acid-substituted phenol relative to the other one. There is apparently a need for more experimental and systematic studies of the effect of H-bond properties on the PCET kinetics in model compounds. Herein we report PCET processes in four new H-bonded tyrosines linked to $Ru^{II}(bpy)_3$ (Chart 1). The phenol groups have internal H-bonds to neutral bases as in PSII, and there is a significant variation in their H-bond lengths. By laser flash/quench kinetic experiments, we examined the relationship between the rate and kinetic isotope effects and the H-bond properties, particularly the proton transfer distance.

Chart 1. Biomimetic Systems of Hydrogen-Bonded Tyrosine Linked to a Photosensitizer

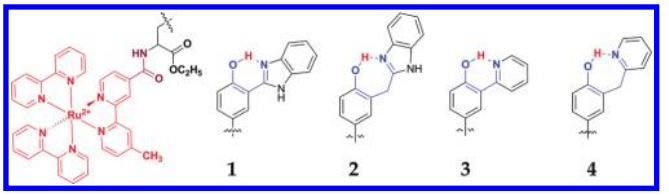

Complexes **1**–**4** (Chart 1) were prepared from tyrosine (**1** and **4**) or tyrosines bearing a halogen substituent (I or Br) at the ortho position (**2** and **3**). The synthesis of **1** started with monoformalation of tyrosine, which was subsequently condensed with *o*-diaminobenzene under an oxygen atmosphere to introduce the benzimidazole group. The nonconjugated benzimidazole in compound **2** was introduced by reaction of

Received: April 15, 2011
Published: August 03, 2011

o-diaminobenzene with 2-bromoethynyltyrosine, which was prepared by a Sonogashira coupling reaction. The pyridyl was introduced at the ortho position of tyrosine by Stille coupling and aldol condensation in the syntheses of **3** and **4**, respectively. Finally, the tyrosines bearing different bases were coupled to $Ru(bpy)_3^{2+}$ via an amido linkage. The final complexes **1**−**4** were fully characterized by NMR spectroscopy and mass spectrometry, and the synthetic details are shown in the SI.

Hydrogen bonding. The ^{1}H NMR spectra of **1**−**4** all show resonance shifts for the phenolic proton between 10.19 and 14.13 ppm (Table 1), consistent with an intramolecular hydrogen bond. The δ_H for **1** and **3** appear at lower fields than those for the corresponding nonconjugated compzounds **2** and **4**. Similar results for related compounds were ascribed to a resonance-assisted H-bond due to conjugation between the phenol and the basic site.[7d] On the basis of the ^{1}H NMR shifts, we do conclude, however, that the H-bond lengths in **1** and **3** are *shorter* than those in their nonconjugated counterparts. This is also supported by the X-ray crystal structures of the analogous phenol−base compounds **1′**−**4′** that are not linked to a Ru complex[11] (see the SI). Thus, the proton transfer distance in the PCET process should be shorter in **1** and **3** than in **2** and **4**.

Electrochemistry and PCET driving force. The electrochemical behavior of **1**−**4** was studied by both cyclic voltammetry and differential pulse voltammetry (DPV) in acetonitrile (Figure 1; Figure S2 and Table S1 in the SI). On the cathodic side of the cyclic voltammogram (CV) during the scan down to −2.5 V (all potentials are vs $Fc^{+/0}$), three redox waves typical for the reduction of the three ligands in $[Ru(bpy_3)]^{2+}$ were observed. At +0.932 V, the reversible $Ru^{III/II}$ oxidation was observed. No electronic influence of the H-bonded tyrosine on the potentials for ligand reduction and $Ru^{III/II}$ oxidation was observed. The most interesting feature of the CV is the irreversible oxidation below the $Ru^{III/II}$ potential, corresponding to oxidation of the phenol group. The peak potentials for this oxidation in differential pulse voltammetry were +0.680, +0.489, +0.720, and +0.570 V for **1**−**4**, respectively. The relative values are in excellent agreement (±10 mV) with those reported for the analogous series of phenols **1′**−**4′**, which gave reversible oxidations in their CVs.[7c,d] The shift toward a less positive potential for **1**−**4** relative to the methylated Ru-TyrOMe (+1.264 V; Table S1) can be ascribed to a PCET process on the electrode with proton transfer to the base, consistent with previous examples of intramolecular phenol−base systems.[7] Notably, the lower potential in the presence of a base is not due to H-bonding per se but arises from a protonation equilibrium with the nearby base, for which the pK_a of the protonated base is the important parameter.[7b] According to the electrochemistry data, the driving force for the concerted PCET process in the nonconjugated tyrosines in **2** and **4** is larger than in their conjugated counterparts in **1** and **3** (Table 1).

Kinetics of intramolecular TyrOH···B oxidation. The intramolecular PCET reaction between TyrOH···B and Ru^{III} was triggered by the flash/quench method, as described in our previous work.[8] Excitation of the $[Ru(bpy)_3]^{2+}$ unit with a 5 ns, 460 nm laser pulse followed by oxidative quenching with methyl viologen $[MV(PF_6)_2]$ gave the corresponding Ru^{III} complex. This was seen from the rapid appearance of $MV^{+\bullet}$ absorption at 390 and 600 nm and bleaching of the Ru^{II} ground state at ∼450 nm (Figure 2a). The subsequent intramolecular PCET between the TyrOH···B and Ru^{III} units was monitored using the recovery of Ru^{II} absorption at 450 nm. The rate constants at different temperatures were also determined from the kinetic traces (Figure 2b) and are plotted in Figure S3. It is striking that the rate constants for **2** and **4** were markedly lower than for **1** and **3** in spite of the significantly larger (0.15−0.20 eV) reaction driving force for **2** and **4**. This will be discussed further in the following sections.

Mechanistic analysis. There are three possible mechanisms for the intramolecular PCET process. A first possibility is electron transfer (ET) from tyrosine to Ru^{III} to form the radical cation Ru^{II}−$TyrOH^{+\bullet}$···B followed by proton transfer (PT) to the base in a stepwise mechanism (the ETPT mechanism). A second stepwise mechanism would involve pre-equilibrium proton transfer to yield the zwitterion Ru^{III}−$TyrO^-$···$^+$HB) followed by electron transfer (the PTET mechanism). The third possibility is concerted electron−proton transfer (CEPT) in a single step with a common transition state. The experimental results show that intramolecular PCET in the present complexes proceeds by the concerted pathway without the involvement of either of the high-energy intermediates Ru^{II}−$TyrOH^{+\bullet}$···B or Ru^{III}−$TyrO^-$···$^+$HB. First, primary kinetic isotope effects (KIEs) k_H/k_D = 1.5−4.0 were found for **1**−**4**. Neither rate-limiting electron transfer (ETPT) nor pre-equilibrium proton transfer (PTET) is consistent with the large values for **2** and **4**. Second, the CEPT mechanism is strongly favored because of its significant driving force (Table 1). In contrast, for the first step in the ETPT mechanism, ΔG°_{ET} can be estimated as +33 kJ mol^{-1} ($K_{ET} = 2.4 \times 10^{-6}$).[12] Additionally, the substituent effect makes the conjugated phenols in **1** and **3** harder to oxidize to the radical cation than the other two phenols. Thus, their PCET rate constants would be smaller than those in **2** and **4** if that mechanism were operative, but instead they are larger. Also, the initial PT is strongly endergonic because of the large pK_a difference between phenol and the bases. On the basis of the pK_a values of benzimidazole (∼17), pyridine (12.3), and phenols (∼27),[13] K_{PT} is expected to be $10^{-14.7}$ to 10^{-10}. The PTET rate constant is the product of K_{PT} and k_{ET}, the rate constant for ET from the zwitterion to Ru^{III}.

Table 1. Experimental Data for 1−4

compound	δ_H (ppm)[a]	k_H (10^5 s^{-1})[b]	KIE[c]	ΔG°_{rxn} (eV)[d]	E_a (kcal/mol)[e]	$d_{O\cdots N}$ (Å)[f]
1	13.04	6.30 ± 0.03	1.42	−0.252	6.11	2.539[g]
2	10.19	0.93 ± 0.01	4.01	−0.443	8.13	2.752[h]
3	14.13	3.81 ± 0.01	2.16	−0.212	6.62	2.567[i]
4	10.71	1.78 ± 0.01	4.02	−0.363	7.32	2.691[i]

[a] ^{1}H NMR shift of the phenolic proton in dry CD_3CN. [b] PCET rate constant at 298 K in acetonitrile with 0.75% H_2O (v/v). [c] Kinetic isotope effect; reactions with deuterated substrates were performed in acetonitrile with 0.75% D_2O (v/v). [d] Calculated from DPV data using the equation $-\Delta G^\circ_{rxn} = e[E^\circ(Ru^{III/II}) - E^\circ(TyrO^\bullet\cdots{}^+HB/TyrOH\cdots B)]$. [e] Activation energies obtained from fits to the Arrhenius equation (Figure S3). [f] Proton donor−acceptor distances from crystallographic data for the related systems **1′**−**4′** (see the SI). [g] Reference 7c. [h] This work (see the SI). [i] Reference 7d.

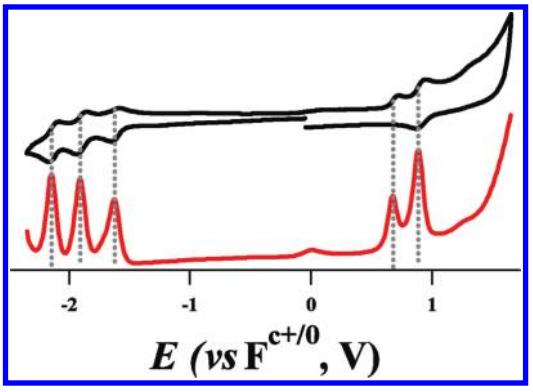

Figure 1. Cyclic voltammogram (black) and differential pulse voltammogram (red) for **3** in acetonitrile with 0.1 M $TBAPF_6$ as the electrolyte, $AgNO_3$/Ag as the reference electrode, and a scan rate of 0.1 V/s.

The observed rate constant $k_{obs} > 10^5\ s^{-1}$ for **1**−**4** then would imply $k_{ET} > 10^{15}\ s^{-1}$, which is far too large to be realistic. Moreover, the reaction would be several orders of magnitude faster with benzimidazole than with pyridine, and this is not observed. On the basis of this discussion, the concerted mechanism is the most likely pathway for **1**−**4**, since this mechanism avoids the involvement of high-energy intermediates (i.e., the radical cations or zwitterions).

Effect of the H-bond properties on the PCET kinetics. Although the PCET driving force in **2** and **4** is significantly larger than in the corresponding complexes **1** and **3**, the observed rate constants are smaller. This cannot be explained simply by the difference in the *strengths* of the conjugated and nonconjugated H-bonds, as discussed in our previous work.[8b,c] Generally, H-bonds are often classified as *strong* or *weak*, and these two types of H-bond are also described as *short* or *long*, respectively. However, the reliability of the relationship between the strength and the length of H-bonds is now in question.[14] In the present series of complexes, both X-ray crystallography and ^{1}H NMR analysis showed that the conjugated phenol−base complexes have shorter H-bonds than their nonconjugated counterparts. The proton donor−acceptor distances $d_{O\cdot\cdot N}$ vary from 2.54 to 2.75 Å (Table 1), and typical O−H and N−H bond lengths are 0.97 and 1.03 Å, respectively, in this type of compound.[15] Thus, the proton tunneling distance (d) should be 0.5−0.8 Å, increasing in the order **1** < **3** < **4** < **2**.

Concerted PCET can be described as a double tunneling at the transition state using a formalism corresponding to that for electron transfer (nonadiabatic regime, eq 1; contributions from vibrationally excited states of O−H and other high-frequency modes are neglected at the present level of discussion[8c,10]). The vibronic coupling V_{PCET} can be treated as the product of the electron and proton couplings (eq 2), where the latter (V_{PT}) is determined by the overlap between the donor- and acceptor-state proton vibrational wave functions. This overlap is strongly dependent on the proton transfer distance d; in a limited range around a chosen reference distance d_0, the overlap decreases exponentially (eq 3).[10,16] Because a deuteron, which is more massive, has a more localized wave function than a proton, deuteron transfer is typically slower and shows a stronger distance dependence, giving rise to a distance-dependent KIE.

$$k_{PCET} = \frac{2\pi}{\hbar}\frac{{V_{PCET}}^2}{(4\pi\lambda RT)^{1/2}}\exp\left[-\frac{(\Delta G^0 + \lambda)^2}{4\lambda RT}\right] \quad (1)$$

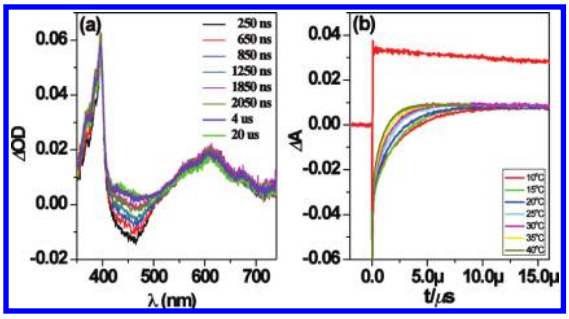

Figure 2. Laser flash/quench-induced transient absorption of complex **1** in the presence of 40 mM $MV^{2+}(PF_6)_2$. (a) Transient absorption spectra at 250, 650, 850, 1250, 1850, 2050, 4000, and 20000 ns after the laser flash. The absorptions at 600 and 390 nm are due to the formation of $MV^{+\bullet}$ in the first quenching step, and the bleaching at 450 nm is due to oxidation of Ru^{II} to Ru^{III}; this absorption recovers on a microsecond time scale due to PCET from the appended tyrosine. (b) Transient absorbance traces at different temperatures showing the rapid generation of the $MV^{+\bullet}$ radical cation at 600 nm (upper trace) and the kinetics of Ru^{II} ground-state absorption recovery at 450 nm (lower traces).

$$V_{PCET} \approx V_{ET}V_{PT} \quad (2)$$

$$V_{PT} = V_{PT}^0 \exp\left[-\frac{\beta}{2}(d - d_0)\right] \quad (3)$$

In the present complexes, we have noted the striking trend of lower rates for the complexes with the larger driving force; this apparently contradicts eq 1 (with $-\Delta G^0 < \lambda$) and requires an explanation. On the other hand, there are obvious differences in $d_{O\cdot\cdot N}$ in the series, with a parallel trend in the KIEs. The complexes with longer $d_{O\cdot\cdot N}$ values show lower PCET rate constants (consistent with eqs 1−3) as well as larger KIEs. To explain our data, we therefore focus on the dependence of k_{PCET} on the two experimentally determined parameters ΔG^0 and d. Thus, at the present level of analysis, we ignore possible differences in the reorganization energy λ and the compressibility (force constant) of the H-bond[8c,10] within this series of complexes (see the SI). When the driving force is small compared with λ and the temperature is constant, eq 1 can be rewritten as eq 4.[17] Inclusion of the second term on the left-hand side compensates for the difference in the reaction free energies of the complexes and allows a better analysis of the dependence of the rate on d. Furthermore, we use the experimental values of $d_{O\cdot\cdot N}$, which should closely track the differences in the tunneling distance d for the compounds. With these approximations, the last term can be treated as a constant for this series of complexes at 298 K.

$$\ln k_{PCET} + \frac{\Delta G^0}{2RT} = -\beta d_{O\cdot\cdot N} + \text{constant} \quad (4)$$

A plot of the data and a linear fit according to eq 4 show very good agreement (Figure 3). The slope parameter β is ∼27 $Å^{-1}$, which shows the large sensitivity of the PCET rate to $d_{O\cdot\cdot N}$ and thus to the tunneling distance d; the variation in the estimated rate constant at equal driving force is nearly 3 orders of magnitude for a difference of only ∼0.2 Å in d. This is in sharp contrast to electron tunneling, for which the distance-dependence parameter β is typically ∼1 $Å^{-1}$.[18] The value of β is in very good agreement with what is theoretically predicted for proton transfer reactions[16a] and PCET.[16c] To the best of our knowledge, this is the first direct

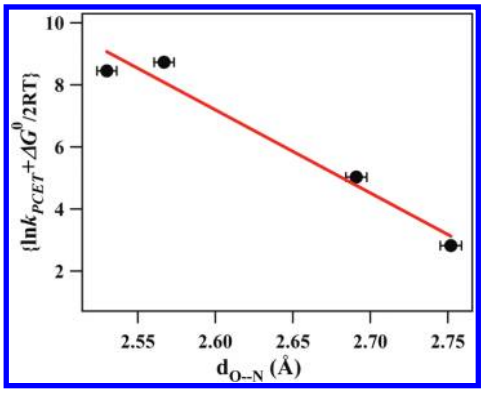

Figure 3. Dependence of the estimated PCET rate constant at $\Delta G^0 = 0$ on the proton donor−acceptor distance d_{O-N}. The red line is a fit to eq 4 (see the text).

experimental demonstration of the dependence of the concerted PCET rate constant on the proton transfer distance for a series of more than two synthetic model complexes.

In conclusion, complexes **1** and **3** with a conjugated base attached to the phenol moiety show a higher rate of concerted PCET than the corresponding nonconjugated ones **2** and **4**, in spite of a larger driving force in the latter. When corrected for differences in driving force, the rate constants differ by 2−3 orders of magnitude. On the basis of the good correlation in Figure 3, this is predominantly due to the shorter H-bond length in **1** and **3**, which gives a shorter proton transfer distance and thus better overlap of the proton wave functions. This is also reflected in the KIE values, which are significantly higher for **2** and **4**. Further experiments and detailed theoretical analysis of the H-bond properties and other parameters governing the PCET rate constant are in progress. The dramatic effect on the PCET rate of small geometric differences as illustrated here emphasizes the importance of carefully controlling the proton transfer component of PCET and H-bonding in both enzymes and the design of efficient molecular catalysts for water splitting and solar fuels production.

■ ASSOCIATED CONTENT

Supporting Information. Synthetic details for **1**−**4**, experimental details for electrochemistry and laser flash photolysis, and crystallographic data (CIF). This material is available free of charge via the Internet at http://pubs.acs.org.

■ AUTHOR INFORMATION

Corresponding Author
Leif@fotomol.uu.se

■ ACKNOWLEDGMENT

We thank Dr. Xue-Li Geng for the help with the growth of a single crystal of compound **2′** and Dr. Marie-Pierre Santoni for X-ray crystallography. This work was supported by the Swedish Research Council, the Swedish Energy Agency, and the Knut and Alice Wallenberg Foundation.

■ REFERENCES

(1) (a) Cukier, R. I.; Nocera, D. G. *Annu. Rev. Phys. Chem.* **1998**, *49*, 337. (b) Decornez, H.; Hammes-Schiffer, S. *J. Phys. Chem. A* **2000**, *104*, 9370. (c) Mayer, J. M. *Annu. Rev. Phys. Chem.* **2004**, *55*, 363. (d) Reece, S. Y.; Nocera, D. G. *Annu. Rev. Biochem.* **2009**, *78*, 673. (e) Huynh, M. H. V.; Meyer, T. J. *Chem. Rev.* **2007**, *107*, 5004. (f) Costentin, C. *Chem. Rev.* **2008**, *108*, 2145. (g) Hammarström, L.; Styring, S. *Philos. Trans. R. Soc., B* **2008**, *363*, 1283.

(2) (a) Hoganson, C. W.; Babcock, G. T. *Science* **1997**, *277*, 1953. (b) Rappaport, F.; Lavergne, J. *Biochim. Biophys. Acta* **2001**, *1503*, 246. (c) Dau, H.; Haumann, M. *Photosynth. Res.* **2007**, *92*, 327.

(3) (a) Babcock, G. T.; Wikström, M. *Nature* **1992**, *356*, 301. (b) Ferguson-Miller, S.; Babcock, G. T. *Chem. Rev.* **1996**, *96*, 2889.

(4) (a) Peters, J. W.; Lanzilotta, W. N.; Lemon, B. J.; Seefeldt, L. C. *Science* **1998**, *282*, 1853. (b) Nicolet, Y.; Piras, C.; Legrand, P.; Hatchikian, E. C.; Fontecilla-Camps, J. C. *Structure* **1999**, *7*, 13.

(5) (a) Burgess, B. K.; Lowe, D. J. *Chem. Rev.* **1996**, *96*, 2983. (b) Rees, D. C.; Howard, J. B. *Curr. Opin. Chem. Biol.* **2000**, *4*, 559.

(6) Stubbe, J.; Nocera, D. G.; Yee, C. S.; Chang, M. C. Y. *Chem. Rev.* **2003**, *103*, 2167.

(7) (a) Rhile, I. J.; Mayer, J. M. *J. Am. Chem. Soc.* **2004**, *126*, 12718. (b) Rhile, I. J.; Markle, T. F.; Nagao, H.; Dipasquale, A. G.; Lam, O. P.; Lockwood, M. A.; Rotter, K.; Mayer, J. M. *J. Am. Chem. Soc.* **2006**, *128*, 6075. (c) Markle, T. F.; Rhile, I. J.; Dipasquale, A. G.; Mayer, J. M. *Proc. Natl. Acad. Sci. U.S.A.* **2008**, *105*, 8185. (d) Markle, T. F.; Mayer, J. M. *Angew. Chem., Int. Ed.* **2008**, *47*, 738. (e) Costentin, C.; Robert, M.; Saveant, J.-M. *J. Am. Chem. Soc.* **2006**, *128*, 4552. (f) Costentin, C.; Robert, M.; Saveant, J.-M. *J. Am. Chem. Soc.* **2007**, *129*, 9953. (g) Fecenko, C. J.; Thorp, H. H.; Meyer, T. J. *J. Am. Chem. Soc.* **2007**, *129*, 15098.

(8) (a) Sjödin, M.; Irebo, T.; Utas Josefin, E.; Lind, J.; Merenyi, G.; Åkermark, B.; Hammarström, L. *J. Am. Chem. Soc.* **2006**, *128*, 13076. (b) Irebo, T.; Johansson, O.; Hammarström, L. *J. Am. Chem. Soc.* **2008**, *130*, 9194. (c) Johannissen, L. O.; Irebo, T.; Sjödin, M.; Johansson, O.; Hammarström, L. *J. Phys. Chem. B* **2009**, *113*, 16214.

(9) (a) Sun, L.; Burkitt, M.; Tamm, M.; Raymond, M. K.; Abrahamsson, M.; LeGourriérec, D.; Frapart, Y.; Magnuson, A.; Kenéz, P. H.; Brandt, P.; Tran, A.; Hammarström, L.; Styring, S.; Åkermark, B. *J. Am. Chem. Soc.* **1999**, *121*, 6834. (b) Lachaud, F.; Quaranta, A.; Pellegrin, Y.; Dorlet, P.; Charlot, M. F.; Un, S.; Liebl, W.; Aukauloo, A. *Angew. Chem., Int. Ed.* **2005**, *44*, 1536. (c) Moore, G. F.; Hambourger, M.; Gervaldo, M.; Poluektov, O. G.; Rajh, T.; Gust, D.; Moore, T. A.; Moore, A. L. *J. Am. Chem. Soc.* **2008**, *130*, 10466. (d) Moore, G. F.; Hambourger, M.; Kodis, G.; Michl, W.; Gust, D.; Moore, T. A.; Moore, A. L. *J. Phys. Chem. B* **2010**, *114*, 14450.

(10) Soudackov, A.; Hatcher, E.; Hammes-Schiffer, S. *J. Chem. Phys.* **2005**, *122*, No. 014505.

(11) HOAr−Bzim (**1′**), HOAr−py (**3′**), and HOAr−CH_2py (**4′**) were reported by Mayer and co-workers,[7b−d] and HOAr−CH_2Bzim (**2′**) was synthesized and characterized in this study (see the SI).

(12) This estimate uses $E(\mathrm{TyrOH^{+\bullet}\cdots B/TyrOH\cdots B}) = 1.264$ V vs $Fc^{+/0}$, which is taken to be same as $E(\mathrm{TyrOMe^{+\bullet}/TyrOMe})$.

(13) We directly use the pK_a values of benzimidazole and pyridine for the analysis and also assume that the pK_a of tyrosine in acetonitrile is similar to those of the phenols without considering the effect of intramolecular H-bonding on the pK_a's of tyrosine and the base. The pK_a values were taken from: Izutsu, K. *Acid-Base Dissociation Constants in Dipolar Aprotic Solvents*; Blackwell: London, 1990.

(14) Perrin, C. L. *Acc. Chem. Res.* **2010**, *43*, 1550.

(15) Allen, F. H.; Kennard, O.; Watson, D. G. *J. Chem. Soc. Perkin Trans. 2* **1987**, S1.

(16) (a) Kiefer, P. M.; Hynes, J. T. *J. Phys. Chem. A* **2004**, *108*, 11793. (b) Kiefer, P. M.; Hynes, J. T. *J. Phys. Chem. A* **2004**, *108*, 11809. (c) Skone, J. H.; Soudackov, A. V.; Hammes-Schiffer, S. *J. Am. Chem. Soc.* **2006**, *128*, 16655.

(17) From eq 1, $\partial(\ln k_{PCET})/\partial(\Delta G^0) = (2RT)^{-1}(1+\Delta G^0/\lambda) \approx (2RT)^{-1}$ when $\Delta G^0 \approx 0$.

(18) (a) Paddon-Row, M. N. In *Electron Transfer in Chemistry*; Balzani, V., Ed.; Wiley-VCH: Weinheim, Germany, 2001; Vol. III, Part 2, Chapter 1, pp 201−215. (b) Gray, H. B.; Winkler, J. R. *Proc. Natl. Acad. Sci. U.S.A.* **2005**, *102*, 3534.